Experimental Determination and Correlation of Artemisinin's Solubility in Supercritical Carbon Dioxide

Patrícia Coimbra,[†] Miguel R. Blanco,[†] Hélio S. R. Costa Silva,[‡] Maria H. Gil,[†] and Hermínio C. de Sousa*,[†]

Departamento de Engenharia Química, Faculdade de Ciências e Tecnologia, Universidade de Coimbra, Pólo II, Pinhal de Marrocos, 3030-290 Coimbra, Portugal, and Faculdade de Ciências Farmacêuticas, USP, Avenue Professor Lineu Prestes 580, Bloco 13, 05508-900, São Paulo, SP, Brazil

The measurement and correlation of the experimental solubility of the antimalarial artemisinin (*Artemisia annua* L.) in supercritical carbon dioxide is reported. Results were obtained using a static analytical method at 308.2, 318.2, and 328.2 K, and in a pressure range from 10.0 up to 25.0 MPa. Solubility experimental data were correlated with three density-based models (Chrastil, Bartle, and Méndez-Santiago−Teja models) and with two cubic equation of state (EOS) models, namely, the Peng−Robinson EOS and the Soave−Redlich−Kwong EOS, together with the conventional van der Waals mixing and combining rules. Good correlation results were obtained between the calculated and the experimental solubility to all fitted models. Results clearly show the feasibility of processing this antimalarial drug using supercritical fluid technologies and processes.

Introduction

Solvents and processes in solution play a central role in the majority of chemical and pharmaceutical industrial processes. The pharmaceutical industry is one of the major industries worldwide and wherein, for comprehensible reasons, safety and ecological considerations on the use of volatile organic solvents (VOCs) and other harmful solvents must be seriously taken into account. The actual severe regulations on the use of these solvents and on their residual level in the final products are a major limitation to most of the traditional pharmaceutical processes. Likewise, both the generation of polluted aqueous waste streams and the energy used to remove water (or other solvents) from final or intermediate products (i.e., drying steps) make important contributions to global pollution. As such, it seems obvious that there are economical, safety, and ecological reasons and a real need to consider, innovate, and optimize either organic solvent-free pharmaceutical processes or the use of "green and environmental friendly" solvents. Supercritical fluids (SCFs) have already proved to be an excellent alternative to replace VOCs, harmful solvents, and other additives in many types of chemical and pharmaceutical process operations. Furthermore, SCFs also present unique properties that may improve these processes as well as offer new and innovative possibilities for the development of new products, with better chemical, physical, morphological, and mechanical properties and, consequently, leading to novel and improved final pharmaceutical applications and products. In recent years, several reviews of pharmaceutical processing (studied systems and applied techniques) using SCFs have been published, demonstrating the existing opportunities offered by these processes and technologies.[1−5]

Carbon dioxide is the most used SCF due essentially to its relatively low critical temperature and critical pressure (T_c = 304.3 K, P_c = 73.7 bar), nontoxicity, noninflammability, and low cost. Because of these favorable properties combined with other typical properties of SCFs like their low viscosities, high diffusivities, and liquid-like densities, supercritical carbon dioxide ($scCO_2$) has found many uses in the nutraceutical and pharmaceutical fields, where its nontoxic nature displays a great advantage. Moreover, its low critical temperature permits supercritical processing at mild temperature conditions, avoiding the possible degradation of thermally labile substances (like most pharmaceuticals and nutraceuticals). Another important advantage is that the elimination of residual solvent is complete, and the recovery of final products is easier and cheaper when compared with many traditional processes. Extraction and separation of natural products,[6−8] recrystallization and drug particle formation,[9−12] preparation of sustained drug delivery systems,[13−15] and as a solvent for pharmaceutical synthesis and enzymatic catalysis[16−18] are some examples of $scCO_2$ potential applications in the pharmaceutical, cosmetics, and nutraceutical industries.

Artemisinin (Figure 1), also known by the chinese name Quinghaosu, is an endoperoxide sesquiterpene lactone produced by the aerial parts of *Artemisia annua* L. (Asteraceae, formerly Compositae), which has been used as a potential and effective antimalarial agent to vitiate the impact of multidrug resistant strains of the malarial parasites, *Plasmodium falciparum* and *Plasmodium vivax*, including the human cerebral malaria.[19−23] In addition, ethanolic extracts of *A. annua* L. also proved to be antiulcerogenic and antitumoral, and its essential oils can be used as repellents, bactericides, and antioxidants.[8] Recently, artemisinin and some of its derivatives also showed a strong antifungal activity against the opportunistic pathogen *Cryptococcus neoformans*.[24]

Although the chemical synthesis of this drug and of its derivatives (dihydroartemisinin, artemether, arteether, artesunic acid, and artelinic acid) is already possible, the synthetic products are not yet as competitive in price as the natural ones, obtained by extraction and isolation from *A. annua* L.[25−27] On the other hand, apparently the pharmaceutical industry is not interested in investing and producing antimalarial drugs because

* To whom correspondence should be addressed. E-mail: hsousa@eq.uc.pt. Fax: +351 239 798703.
[†] Universidade de Coimbra.
[‡] USP.

10.1021/je060015y CCC: $33.50
Published on Web 04/26/2006

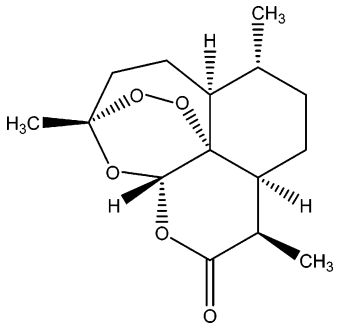

Figure 1. Chemical structure of artemisinin (*Artemisia annua* L.).

most of the infected people live in nondeveloped and developing countries, where the pharmaceutical market is not attractive enough, and there is insufficient patent protection.[28] Therefore, the most used method to obtain artemisinin is by liquid organic solvent extraction from *A. annua* L. dried aerial parts (leaves, stems, buds, and flowers). Typical employed solvents are toluene, *n*-hexane, cyclohexane, ethanol, chloroform, and petroleum ether.[29−31] Microwave-assisted liquid solvent extraction was also employed in order to increase liquid extraction rates.[31,32] However, and in general, the extracts obtained by liquid solvent extraction contain large amounts of undesired compounds such as chlorophyll and other organic molecules. This will decrease the extraction selectivity and will introduce difficulties in the drug purification process, leading to low extraction yields.[8] Moreover, its peroxide bridge, which is essential for its activity, is very reactive and may react with compounds used in the purification of extracts. Finally, liquid solvent extractions frequently require dehydrated or dried plant material, and it is well-established that the employed drying methods can have a strong influence on the final artemisinin recovery.[31] Recently, $scCO_2$ extraction proved to be a promising alternative to extract artemisinin from the dried plant material.[8,33,34] Supercritical technology was also used to produce artemisinin particles by rapid expansion of supercritical solutions (RESS), which showed improved dissolution properties.[9]

However, for the design of any pharmaceutical process based in SCF technology (SCF extraction, drug particle formation SCF techniques, etc.), the accurate knowledge of the equilibrium solubility data, in different conditions of temperature and pressure, between the pharmaceutical compounds of interest and the SCF solvent is required. Performing a quick search through the literature, one can easily find data on the solubility (in $scCO_2$) of several drugs and other biomolecules of pharmaceutical interest, determined using different experimental methods.[2−5,10−12,35−42] Modeling and correlation of the solubility of solids in $scCO_2$ were also extensively investigated.[43−51]

Solid solubilities in SCFs (and drug solubilities in particular) are not easy to predict because there is a lack of accurate models to simulate and predict equilibrium solubilities of these compounds in SCFs and there is not much information regarding most physical properties necessary for those available models. Furthermore, when applying these predictive models, other complications may come up like, for example, their failure because these mixtures are usually very asymmetric in terms of size and energy differences between the components: for example, solid solute molecules are usually large and polar (like most drugs) while supercritical solvent molecules are usually small and show low polarity (like CO_2).[51]

If not completely predicted or determined experimentally, drug solubility in SCFs must be obtained and extended through correlations based on theoretical or empirical models applied to the existing experimental data. Generally, the most common models used for correlating solid-supercritical phase equilibria are cubic equations of state (EOSs), noncubic EOSs, activity coefficient models, and semiempirical correlations based on density, pressure, and temperature.[52] Undoubtedly, the most used models are cubic EOSs from the van der Waals family, like the Peng−Robinson[53] (PR) and Soave−Redlich−Kwong[54] (SRK) EOSs, together with several mixing and combining rules, like the classical van der Waals mixing rules (vdW). The above referred EOS models require one or more temperature-dependent interaction parameters that must be correlated from the experimental solubility data. In addition, EOS models need data on several critical and other physicochemical properties of solutes that are not always available in the literature, mainly for pharmaceutical compounds and other less common substances. In general, these solid's properties (critical properties, molar volume, sublimation pressure, and Pitzer's acentric factor) are not yet experimentally determined and have to be predicted by several estimation and group-contribution methods (sometimes not very reliable). Consequently, this may introduce additional errors on the correlation results or may originate very unlike adjusted parameters results, depending on the applied methods. Therefore, extreme caution should be taken when choosing and applying these estimation methods. To avoid some of these difficulties as well as more complicated computational routines, most authors decide to use several empirical correlations such as density-based correlations[43−45] (Chrastil, Bartle, and Méndez-Santiago−Teja models) or the Ziger−Eckert semiempirical correlation.[50] These models are based on simple error minimization using least-squares methods, and for the majority of them, there is no need to estimate and use critical and thermophysical properties of the involved solids.

Despite the above referred disadvantages and difficulties associated to these correlation models, they are widely employed and normally used to fit and correlate solubility experimental data for a given envisaged practical purpose. Thus, they are very helpful for the development of supercritical applications and processes that require the accurate knowledge of solid solubility in SCFs. However, and like most correlation models, even for other applications, they should be preferably employed just in the experimental data range (i.e., for interpolation of results). Using these models to extrapolate to outside the experimental data range should be performed very carefully (it can be done, but for regions very near to the limits of the experimental data range). Extrapolation for other regions, far from this range, can originate unreliable results.

Only recently the solubility of artemisinin in $scCO_2$ was measured, at four isotherms, correlated and reported,[55] using a flow-type apparatus equipped with a high-pressure UV detector. Correlation on the experimental data was done using a density- and temperature-based equation. In the present work, the equilibrium solubility of artemisinin in $scCO_2$ was measured, from 10.0 up to 25.0 MPa, and at 308.2, 318.2, and 328.2 K, using a static analytical method. Results were compared to the ones obtained by Ren and co-workers.[55] Experimental data were correlated using three different density-based correlations (Chrastil, Bartle, and Méndez-Santiago−Teja models) and by the PR and SRK EOSs, together with the conventional van der Waals mixing and combined rules.

Experimental Section

Materials. Carbon dioxide (CAS 124-38-9) (purity > 99.998 %) was purchased from Praxair, dichloromethane (CAS 75-09-2) (purity > 99.9 %) was obtained from Fluka. Artemisinin

(CAS 63968-64-9) (from Mediplantex, analytical grade) was kindly supplied by Prof. Mitchel A. Avery from the University of Mississipi.

Experimental Procedure. The experimental solubility of artemisinin in $scCO_2$ was measured using a static equilibrium method and following a experimental procedures already described in detail.[5,36,52] A stainless steel equilibrium visual cell, with an internal volume of approximately 30.0 cm^3, was loaded with the solid solute and a magnetic stirrer and immersed in a thermostatic water bath. A ThermoHaake temperature controller maintained the operational temperature within ± 0.1 K. The system was pressurized with CO_2 by means of a high-pressure liquid pump, and the pressure inside the cell was measured with a high-pressure transducer (Setra, model 204, 0.0−34.40 ± 0.04 MPa), calibrated between 0 and 20.5 MPa. When the desired operational temperature and pressure were attained, the solid + CO_2 mixture was stirred during 1 h, for equilibration and fluid phase saturation. We carried out several preliminary experiments in order to determine the amount of solubilized drug as a function of equilibration and saturation time. For this compound, the required saturation time was around 30 min. Nevertheless, we kept the saturation process for 60 min (with strong stirring) plus a 20 min period without stirring. A sample was then taken, using a six-port sampling valve (Rheodyne high-pressure switching valve, model 7060) and a sampling loop of approximately 0.5 cm^3. The sample was quickly depressurized and the precipitated solid was collected in a small glass trap. The gas in the sample was expanded into a large precalibrated volume, composed by a glass trap (15.9 cm^3) and a metal balloon (1735.05 cm^3), and previously brought into sub-atmospheric pressure. The amount of CO_2 in the sample was calculated based on the resulting sub-atmospheric pressure increase, which was measured with a high precision low-pressure transducer (Setra, model 204, $0.0-0.175 \pm 1.9 \times 10^{-4}$ MPa). To ensure that all solute was recovered, a cleaning solvent (dichloromethane) was injected through the sample loop and the expansion lines and recollected in the glass trap. Lines were also cleaned with fresh CO_2, smoothly pressurized.

Analytical Method. The amount of solubilized solid drug was determined by spectrophotometric UV analysis. The collected samples, containing the solid drug, were diluted in dichloromethane to a convenient volume, and the absorbancies of the resulting sample solutions were measured, at fixed wavelength (229 nm), by a UV/VIS spectrophotometer (JASCO V-530). Calibration curve was obtained by UV analysis of previously prepared standard samples, with concentrations between 0.5 and 3 mg/mL.

For each sample, the amount of CO_2 was calculated using the Virial EOS (applied to pure CO_2), the values of the precalibrated expansion volumes, the resulting sub-atmospheric pressure increase due to expansions, the temperature of the water bath (± 0.01 K), and the temperature of the glass trap (which was considered to be 273.15 K).

Correlation of Experimental Solubility Data

Density-Based Models. The Chrastil model[43] relates the solubility of a solid solute in a SCF as a function of the density of the pure SCF and of the absolute temperature. It is based on the supposition that one molecule of solute, A, associates with k molecules of solvent, B, to form a solvate complex, AB_k, in equilibrium with the system. Taking in consideration several thermodynamic considerations, it is easy to obtain the following expression for the solid solubility in a SCF:

$$\ln S = k \ln \rho + \alpha/\mathrm{T} + \beta \tag{1}$$

In this expression, S ($kg \cdot m^{-3}$) is the solubility of the solid in the supercritical phase; ρ ($kg \cdot m^{-3}$) is the density of the pure supercritical fluid; k is the association number; α is a constant, defined as $\Delta H/R$ (where ΔH is the sum of the enthalpies of vaporization and solvation of the solute and R the gas constant); and β is another constant related to the molecular weight of the solute and solvent. The parameters k, α, and β are obtained performing a multiple linear regression on the obtained experimental solubility data.

Bartle et al.[44] proposed another simple density-based semiempirical model to correlate the solubility of solids in SCFs:

$$\ln\left(\frac{yp}{p_{\mathrm{ref}}}\right) = A + C(\rho - \rho_{\mathrm{ref}}) \tag{2}$$

$$A = a_1 + a_2/T \tag{3}$$

$$\ln\left(\frac{yp}{p_{\mathrm{ref}}}\right) = a_1 + a_2/T + C(\rho - \rho_{\mathrm{ref}}) \tag{4}$$

In these expressions, p_{ref} is assumed as a standard pressure of 0.1 MPa (1.0 bar); ρ_{ref} is a reference density, assumed as 700 $kg \cdot m^{-3}$; and a_1, a_2, A, and C are empirical constants, determined in the following way: from the experimental solubility data, each isotherm is fitted using eq 2, to obtain the values of A and C. In this model, the parameter a_2 is related to the enthalpy of sublimation of the solid solute, ΔH_{sub}, by the expression $\Delta H_{\mathrm{sub}} = -Ra_2$ (R is the gas constant).

Finally, and based on the theory of dilute solutions, Méndez-Santiago and Teja[45] proposed a simple linear expression to correlate the solubility of solids in SCFs:

$$T \ln(yp) = A' + B'\rho + C'T \tag{5}$$

where A', B', and C' are constants, considered as temperature independent, and obtained by a multiple linear regression of solubility experimental data.

EOS-Based Models. The solubility of a solid solute (2) at equilibrium with a fluid at high pressures (1) can be calculated using the following well-known expression:

$$y_2 = \frac{p_2^{\mathrm{sub}}}{p} \frac{1}{\varphi_2^{\mathrm{SCF}}} \exp\left[\frac{v_2(p - p_2^{\mathrm{sub}})}{RT}\right] \tag{6}$$

In this expression, p_2^{sub} is the sublimation pressure of the pure solid at temperature T, v_2 is the molar volume of the solid, and φ_2^{SCF} is the fugacity coefficient of the solid in the fluid phase, which expresses the nonideality of the fluid phase. This fugacity coefficient is usually evaluated using an EOS. In this work, the Peng−Robinson[53] EOS (eq 7) and the Soave−Redlich−Kwong[54] EOS (eq 8) were used:

$$p = \frac{RT}{v - b} - \frac{a}{v(v + b) + b(v - b)} \tag{7}$$

$$p = \frac{RT}{v - b} - \frac{a}{v(v + b)} \tag{8}$$

To use the above EOSs, for a binary solid + SCF mixture, we employed the classical van der Waals (vdW) mixing and

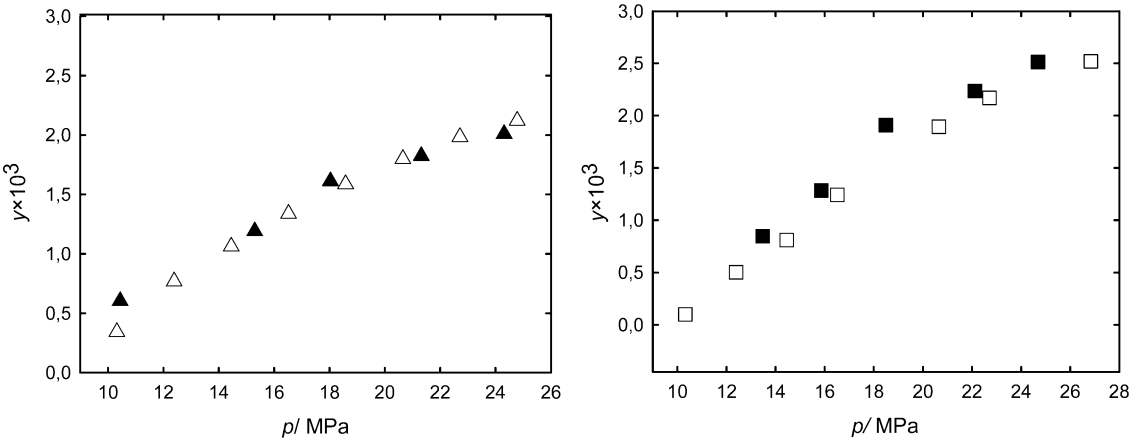

Figure 2. Comparison between this work (filled symbols) and the work reported by Ren et al.[55] (open symbols) at 318.2 K (triangles) and 328.2 K (squares).

Table 1. Experimental Solubility (*y*) of Artemisinin in Supercritical Carbon Dioxide

$T = 308.2$ K			$T = 318.2$ K			$T = 328.2$ K		
p/MPa	ρ/kg·m^{-3}	$y \times 10^3$	p/MPa	ρ/kg·m^{-3}	$y \times 10^3$	p/MPa	ρ/kg·m^{-3}	$y \times 10^3$
10.4	720.7	0.701	10.4	539.2	0.603	13.5	586.9	0.847
13.2	786.5	0.925	15.3	743.9	1.191	15.9	672.2	1.284
16.3	828.5	1.134	18.0	786.5	1.610	18.5	727.4	1.908
18.6	851.0	1.521	21.3	823.3	1.825	22.1	777.8	2.237
21.6	876.3	1.716	24.3	849.3	2.009	24.7	804.7	2.514
25.2	900.4	1.788						

combining rules, with one or with two adjustable parameters, k_{ij} and l_{ij}:

$$a = \sum_i \sum_j y_i y_j (a_i a_j)^{0.5} (1 - k_{ij}) \tag{9}$$

$$b = \sum_i \sum_j y_i y_j \left(\frac{b_i + b_j}{2}\right)(1 - l_{ij}) \tag{10}$$

The binary interaction parameters, k_{ij} and l_{ij}, are obtained by fitting experimental data, through the minimization of an objective function, the average absolute relative deviation (AARD), defined as

$$\text{AARD}/\% = \frac{100}{N} \sum_n \frac{|y^{\text{cal}} - y^{\text{exp}}|}{y^{\text{exp}}} \tag{11}$$

In this equation, N is the number of experimental data points, y^{cal} is the calculated solubilities, and y^{exp} is the experimental solubility data points.

Results and Discussion

The solubility of artemisinin in $scCO_2$ was determined at 308.2, 318.2, and 328.2 K, in the pressure range from 10.0 up to 25.0 MPa, following the method described in the Experimental Section. Results are summarized in Table 1. For each isotherm, experimental data points (at a certain pressure) are an average of, at least, three experimental solubility measurements. Each (p, T, y) data point is accepted if the corresponding standard deviation is less than ± 5 %. The overall uncertainty, taking in consideration the random uncertainties (statistical, associated to Beer−Lambert's calibration curve and to the average of the experimental solubility measurements) and the systematic uncertainties (uncertainties due to the preparation of standard calibration solutions and to pressure and temperature measurements) was found to less than 1.2×10^{-4} (in y, mole fraction of artemisinin).

At the studied conditions, the solubility of artemisinin in $scCO_2$, in terms of mole fraction, ranges from 10^{-4} to 10^{-3}, which is higher than the typical solubilities of many drugs and molecules of biological and pharmaceutical interest. Generally, these compounds have a relatively low solubility, usually around or inferior to 10^{-4}, in terms of mole fraction, at the same investigated pressure range and temperatures.[2−5,10−12,35−42]

It is well-known that the solubility of a solid in a SCF depends essentially on the specific interactions between the solid solute and the SCF as well as on the molecular weight of the solid (and on pressure and temperature). If the SCF is a small nonpolar molecule (like CO_2), one should anticipate that strong polar high molecular weight substances (like most drugs) are hard to dissolve (or even insoluble) in $scCO_2$. From Figure 1, we can see that artemisinin is a large molecule ($M_w = 282.33$ gmol^{-1}), and from its structure, we may expect that it is a strong polar molecule. Polarity can be discussed in terms of the dipole moments of substances. But, dipole moments are not easy to calculate/estimate, and usually it is difficult to find any available and/or consistent values in the literature for this kind of substances. Even when using molecular simulation programs to estimate these values, it is a very difficult task because most drugs possess stereoisomers and each stereoisomer can present several conformers, having different dipole moments.

Artemisinin's dipole moment was found to be around 6.14 D, calculated by a molecular mechanics (MM2) force field model and by a semiempirical molecular orbital model (MOPAC).[56] Therefore, we should expect a low solubility in $scCO_2$ and not a relatively high solubility like the one experimentally observed. Thus, these high solubility values may be due to some specific interactions that may occur between artemisinin and $scCO_2$ like, for example, specific interactions that may take place between its carbonyl group and $scCO_2$.[57−59] Another possible explanation could be the interactions that may happen between the lone pairs of electrons at oxygen atoms of artemisinin (peroxide, ether, and lactone groups) and $scCO_2$. It is known that CO_2 has a large quadrupole moment[60] as a result of its highly electronegative oxygen atoms, and it is credible that it may lead to a favorable quadrupole−dipole interaction between CO_2 and artemisinin.

In Figure 2, we compare our experimental data, at 318.2 K and 328.2 K, with the experimental solubility data previously reported by Ren and co-workers[55] at 318.1 K and 328.1 K, measured with a flow-type apparatus, equipped with a high-pressure UV detector. As can be seen, and despite the different employed experimental methods, our results are in quite good

Table 2. Comparison between the Solubility Data

$T = 308.2$ K				$T = 318.2$ K				$T = 328.2$ K			
p/MPa	$y \times 10^3$ [a]	$y \times 10^3$ [b]	dev/%	p/MPa	$y \times 10^3$ [a]	$y \times 10^3$ [b]	dev/%	p/MPa	$y \times 10^3$ [a]	$y \times 10^3$ [b]	dev/%
10.4	0.783	0.701	10.5	10.4	0.397	0.603	51.9	13.5	0.741	0.847	14.2
13.2	1.096	0.925	15.6	15.3	1.259	1.191	5.4	15.9	1.203	1.284	6.7
16.3	1.348	1.134	15.9	18.0	1.562	1.610	3.1	18.5	1.615	1.908	18.2
18.6	1.502	1.521	1.3	21.3	1.872	1.825	2.5	22.1	2.090	2.237	7.1
21.6	1.693	1.716	1.4	24.3	2.122	2.009	5.3	24.7	2.388	2.514	5.3
25.2	1.895	1.788	5.6								

[a] Obtained by the correlation of Ren and co-workers.[55] [b] Obtained experimentally, this work.

Table 3. Correlated Parameters and Correspondent AARD Values, Obtained from Experimental Data Correlation Using Chrastil, Bartle, and Méndez-Santiago−Teja Models

Chrastil Model, eq 1	
k	4.1
α/K	−3846.1
β	−13.35
ΔH/(kJ·mol^{-1})	−32.0
AARD/%	8.4
Bartle Model, eq 4	
a_1	19.18
a_2/K	−6720.6
C/(m^3·kg^{-1})	0.008
ΔH_{sub}/(kJ·mol^{-1})	55.9
AARD/%	11.6
Méndez-Santiago−Teja Model, eq 5	
A'/K	−8154.5
B'/(K·m^3·kg^{-1})	2.4
C'	26.1
AARD/%	11.8

agreement with the already published data (except for the lower pressure points, where the discrepancy is generally higher).

In the above cited work, Ren and co-workers fitted their experimental solubility data (for four isotherms (310.1 K, 318.1 K, 328.1 K, and 338.1 K) using the correlation:

$$\ln(y) = a \ln(\rho T) + b\rho + c/T + d \qquad (12)$$

They obtained the following fitted parameters (for AARD referred as 4.24 %): $a = 2.162$; $b = 0.002238$; $c = -2795.485$; and $d = -26.311$. In Table 2, we present the calculated artemisinin's solubility using Ren's correlation and fitted parameters (for each temperature and pressure data point), and we compared these results with our experimental values. As referred at the graphical analysis (Figure 2), results are, in general, in good agreement except for lower values of pressure. These differences may be due to the diverse employed experimental methods. A possible cause to these different values may be due the different fluid phase saturation periods used at each method. Ren's method, at lower pressures, just allowed an initial total saturation period of less than 20 min and then pressure was increased in sequential steps, while we used around 80 min of saturation time for every point. Therefore, at 318.2 K and 328.2 K and because of lower fluid phase densities, incomplete saturation can be achieved at these lower pressures, originating lower solubility values than the ones obtained in our work. At 308.2 K, Ren and co-workers did not report the experimental solubility results, but we also determined these values using their correlation. For this isotherm, Ren's correlation originated higher solubility values than the ones obtained in our work (for lower pressures). However, we cannot be sure if their correlation can be confidently used outside the experimental temperature range for which the correlation parameters were determined.

The three density-based (Chrastil, Bartle, and Méndez-Santiago−Teja models) correlation results are presented in Table 3 and represented in Figures 3 to 5. To all the employed models, the quality of the correlation is expressed in terms of the AARD. All the three density-based models were able to successfully correlate the experimental artemisinin + $scCO_2$ solubility data, with AARD values around 8 to 12 %.

As referred in Introduction, cubic EOS models need data on several critical and other physicochemical properties of solutes that are not always available in the literature, namely, critical properties, molar volume, sublimation pressure, and Pitzer's acentric factor. Therefore, these properties have to be predicted by several estimation and group-contribution methods, which

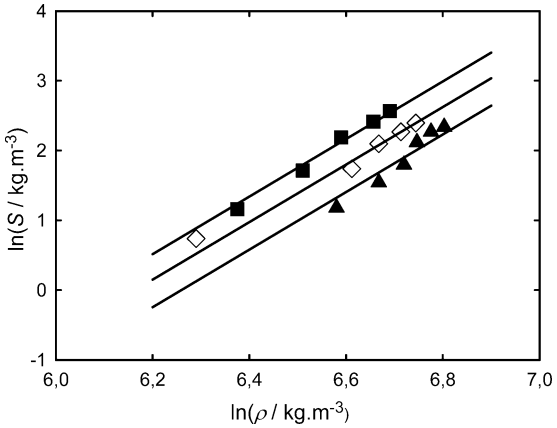

Figure 3. Logarithmic relationship between the solubility of artemisinin in $scCO_2$ and the density of pure CO_2. Experimental: ▲, 308.2 K; ◇, 318.2 K; ■, 328.2 K; —, calculated by eq 1, Chrastil's model.

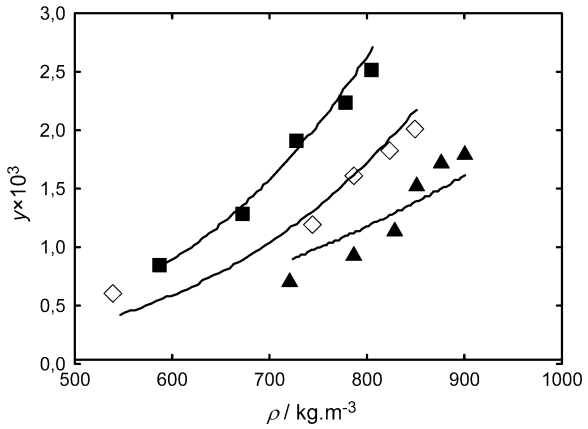

Figure 4. Solubility of artemisinin in $scCO_2$ as a function of the density of pure CO_2. Experimental: ▲, 308.2 K; ◇, 318.2 K; ■, 328.2 K; —, calculated by eq 4, Bartle's model.

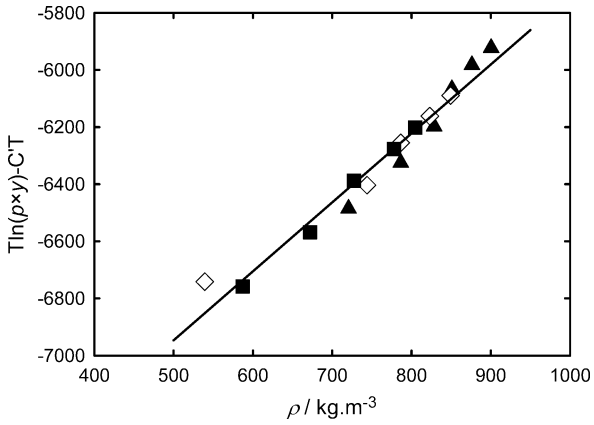

Figure 5. Relationship between the solubility of artemisinin and the density of pure CO_2. Experimental: ▲, 308.2 K; ◇, 318.2 K; ■, 328.2 K; —, calculated by eq 5, Méndez-Santiago−Teja's model.

Table 4. Estimated Critical and Other Required Thermophysical Properties of Artemisinin

T_b	T_c	p_c		$10^6 \times v_2$	$p_2^{sub} \times 10^3$/MPa		
K	K	MPa	ω	$m^3 \cdot mol^{-1}$	308.2 K	318.2 K	328.2 K
560.1[a]	767.7[a]	2.445[a]	0.603[b]	211.5[c]	0.671[b]	1.719[b]	4.110[b]

[a] Estimated by Constantinou−Gani (first-order) method.[61] [b] Estimated by the Ambrose−Walton corresponding states method.[61] [c] Estimated by Fedors' method.[62]

Table 5. Correlation Results for the Solubility of Artemisinin in $scCO_2$, Obtained with the Peng−Robinson and the Soave−Redlich−Kwong Equations of State

		PR-EOS			SRK-EOS		
T/K	mixing rule	k_{12}	l_{12}	AARD/%	k_{12}	l_{12}	AARD/%
308.2	vdW1	0.188		19.0	0.200		21.7
	vdW2	0.250	0.144	6.2	0.270	0.169	6.6
318.2	vdW1	0.184		9.0	0.193		10.8
	vdW2	0.219	0.075	8.4	0.243	0.105	9.1
328.2	vdW1	0.186		9.6	0.196		11.5
	vdW2	0.233	0.100	2.5	0.250	0.120	2.7

sometimes are not very trustworthy. Consequently, this may introduce additional errors on the EOS correlation results or may originate very unlike adjusted parameters results, depending on the applied methods. Therefore, some prudence should be taken when selecting and applying these estimation methods. In some previous work,[51,52] we already discussed the influence of these group-contribution methods on the estimation of these required properties and their consequences on the final EOS correlation results. Accordingly, for artemisinin, these properties were estimated using the group-contribution methods indicated in Table 4.[51,61,62]

In Table 5, we present the optimal fitted binary parameters and the respective AARD values, obtained by experimental data correlation using the PR-EOS and the SRK-EOS, combined with the van der Waals mixing and combining rules, with one adjustable parameter (vdW1) and with two adjustable parameters (vdW2).

Correlation results obtained with the PR-EOS and SRK-EOS, in respect to AARD values, are very similar, both for vdW1 and vdW2 mixing and combining rules. As expected, the best correlations, for both EOSs, were obtained for the vdW2 mixing and combining rule, with two adjustable parameters. Of course, this can be explained by the fact that a model with two adjustable parameters has more "flexibility" to fit the experimental data than a model with only one adjustable parameter, such as vdW1. Figure 6 shows the correlation of experimental solubility data obtained with the PR-EOS, using vdW2 mixing and combining rule. Correlated curves evidence the retrograde solubility behavior characteristic of most of the solid/SCF systems, which is caused by the opposite effect of temperature on the density of the supercritical fluid and on the sublimation pressure of the solid solute. For this system, this so-called "crossover region", where one can observe the intersection of the solubility isotherms, is located between 13.0 MPa and 17.0 MPa.

One of our objectives in determining the experimental solubility of artemisinin in $scCO_2$ carbon dioxide is to make use of the obtained data (experimental and correlated) for the design and development of supercritical processes based on this drug (like particle formation and supercritical solvent impregnation techniques). And, for these purposes, the accurate knowledge of drug solubility and the quality and confidence of the applied correlations is indispensable (for interpolations inside the experimental ranges investigated). To improve the confidence on our correlated results, we must also try to perceive the effect of the overall uncertainty of the experimental data on the correlation results**.** A feasible way to do this is to consider the obtained overall uncertainty associated with all experimental data points and then, "create" two new sets of "experimental" data points: one consisting of their average experimental value added by the overall uncertainty and the other consisting of their average values subtracted by the same overall uncertainty. Subsequently, we must correlate the models, using these two new "experimental" sets of data points. Applying this procedure, we will obtain an "area" in which drug solubility, with some degree of confidence, should be comprised.

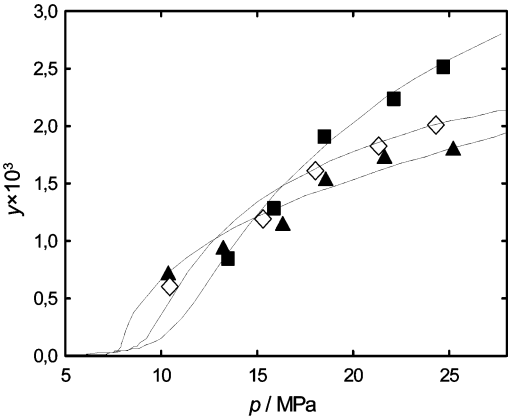

Figure 6. Solubility of artemisinin in $scCO_2$. Experimental: ▲, 308.2 K; ◇, 318.2 K; ■, 328.2 K; −, calculated with the PR-EOS and the vdW2 mixing and combining rule (two adjustable parameters).

Table 6. Correlation Results for the Solubility of Artemisinin in $scCO_2$, Obtained with the PR-EOS, and the vdW2 Mixing and Combining Rule

T		PR-EOS−vdW2		
K		k_{12}	l_{12}	AARD/%
308.2	$y - OU$[c]	0,276	0,189	6,26
	y[a]	0,250	0,144	6,20
	$y + OU$[b]	0,233	0,115	6,15

[a] Applied to the average experimental solubility (y). [b] Applies to the average experimental solubility, added by the overall uncertainty ($y + OU$). [c] Applied to the average experimental solubility, subtracted by the overall uncertainty ($y - OU$).

As an illustrative example of this procedure, we applied the PR-EOS, together with the vdW2 mixing and combining rule (vdW2, with two adjustable parameters), for the experimental results obtained at 308.2 K. Results are summarized in Table 6 and presented in Figure 7.

As can be seen, we will get an area of "probable" drug solubility, as a function of pressure, for each isotherm, which is located between the curves obtained for the correlation of ($y + OU$) and ($y - OU$) data. Interaction parameters showed a relative error (to the experimental average solubility correlated parameters) of 6.8 to 10.4 % (for k_{12}) and 25.2 to 31.3 % (for l_{12}). AARD values are similar for the three performed correlations.

Therefore, this procedure may provide more confidence for the selection of the operational (p, T) conditions to apply in the development of any supercritical process that requires the solubility data of this drug in $scCO_2$. However, as as already referred, this should be employed just in the experimental data range (i.e., for interpolation of results). Similar procedures can be done for other EOS models as well as for the presented density-based models (Chrastil, Bartle, and Méndez-Santiago−Teja models).

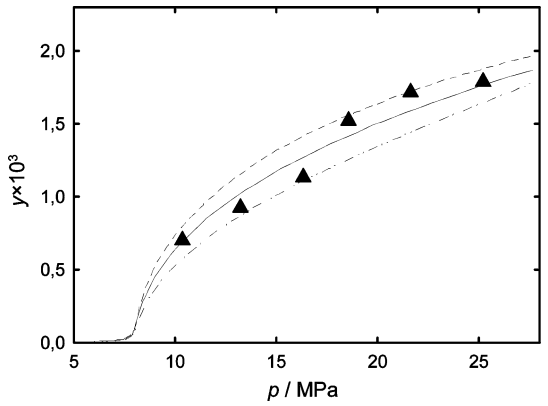

Figure 7. Correlation of artemisinin's solubility in $scCO_2$, at 308.2 K, and using the PR-EOS-vdW2 model. ▲, experimental average solubility; —, calculated for the average experimental solubility (y); - - -, calculated for the average experimental solubility, added by the overall uncertainty (y + OU); — · —, calculated for the average experimental solubility, subtracted by the overall uncertainty (y − OU).

Conclusions

The solubility of artemisinin in $scCO_2$ was measured and correlated at various pressures and temperatures (at 308.2 K, 318.2 K, and 328.2 K, in the pressure range from 10.0 MPa up to 25.0 MPa). Experimental results were compared with those in the existing literature, and good agreement was found despite different experimental methods are different. Results clearly show the feasibility of processing this antimalarial drug using supercritical fluid technologies and processes. Furthermore, these results may be an indication that, possibly, other artemisinin's derivatives will be also soluble in $scCO_2$.

The obtained high solubility values were discussed in terms of possible and potential specific interactions that may occur between artemisinin and $scCO_2$ like, for example, those that may take place between its carbonyl group and $scCO_2$ as well as other interactions which may occur between the lone pairs of electrons at oxygen atoms of artemisinin (peroxide, ether, and lactone groups) and $scCO_2$ (quadrupole−dipole interaction between CO_2 and artemisinin).

Results were correlated with several models found in the literature: three density-based models (Chrastil, Bartle, and Méndez-Santiago−Teja models), and with two cubic EOS models, namely, the PR-EOS and the SRK-EOS, together with the conventional van der Waals mixing and combining rules. All fitted models were shown to be able to successfully correlate experimental solubility data.

The correlation models used in this work proved to be very helpful for the development of supercritical applications and processes that require the precise knowledge of artemisinin's solubility in $scCO_2$. A simple procedure, introducing the effect of the experimental overall uncertainty, was suggested in order to provide more assurance for the selection of the operational (p, T) conditions to apply in the development of these supercritical processes. However and like most correlation models, they should be employed just in the experimental data range (i.e., for interpolation of results). Extrapolation for other regions, far from this range, can originate unreliable results.

Literature Cited

(1) Subramaniam, B.; Rajewski, R. A.; Snavely, K. Pharmaceutical processing with supercritical carbon dioxide. *J. Pharm. Sci.* **1997**, *86* (8), 885−890.

(2) Elvassore, N.; Kikic, I. Pharmaceutical processing with supercritical fluids. In *High-Pressure Process Technology*: *Fundamentals and Applications*; Bertucco, A., Vetter, G., Eds.; Elsevier Science: Amsterdam, The Netherlands, 2001; pp 612−625.

(3) Knez, Z.; Weidner, E. Precipitation of solids with dense gases. In *High-Pressure Process Technology*: *Fundamentals and Applications*, Bertucco, A., Vetter, G., Eds.; Elsevier Science: Amsterdam, The Netherlands, 2001; pp 587−611.

(4) Kompella, U. B.; Koushik, K. Preparation of drug delivery systems using supercritical fluid technology. *Crit. Rev. Ther. Drug Carrier Syst.* **2001**, *18* (2), 173−199.

(5) Jung, J.; Perrut, M. Particle design using supercritical fluids: literature and patent survey. *J. Supercrit. Fluids* **2001**, *20*, 179−219.

(6) McHugh, M.; Krukonis, V. *Supercritical Fluid Extraction*, 2nd ed.; Butterworth-Heinemann: Boston, 1994.

(7) Mukhopadhyay, M. *Natural Extracts Using Supercritical Carbon Dioxide*; CRC Press: New York, 2000.

(8) Quispe-Condori, S.; Sánchez, D.; Foglio, M. A.; Rosa, P. T. V.; Zetzl, C.; Brunner, G.; Meireles, M. A. Global yield isotherms and kinetic of artemisinin extraction from *Artemisia annua* L. leaves using supercritical carbon dioxide. *J. Supercrit. Fluids* **2005**, *36*, 40−48.

(9) Van Nijlen, T.; Brennan, K.; Van den Mooter, G.; Blaton, N.; Kinget, R.; Augustijns, P. Improvement of the dissolution rate of artemisinin by means of supercritical fluid technology and solid dispersions. *Int. J. Pharm.* **2003**, *254*, 173−181.

(10) Bettini, R.; Bonassi, L.; Castoro, V.; Rossi, A.; Zema L.; Gazzaniga, A.; Giordano, F. Solubility and conversion of carbamazepine polymorphs in supercritical carbon dioxide. *Eur. J. Pharm. Sci.* **2001**, *13*, 281−286.

(11) Alessi, P.; Cortesi, A.; Kikic, I.; Foster, N. R.; Macnaughton, S. J.; Colombo, I. Particle production of steroid drugs using supercritical fluid processing. *Ind. Eng. Chem. Res.* **1996**, *35*, 4718−4726.

(12) Velaga, S. P.; Ghaderi, R.; Carlfors, J. Preparation and characterisation of hydrocortisone particles using a supercritical fluid extraction process. *Int. J. Pharm.* **2002**, *231*, 155−166.

(13) Charoenchaitrakool, M.; Dehghani, F.; Foster, N. R. Utilization of supercritical carbon dioxide for complex formation of ibuprofen and methyl-β-cyclodextrin. *Int. J. Pharm.* **2002**, *239*, 103−112.

(14) Okamoto, H.; Sakakura, Y.; Shiraki, K.; Oka, K.; Nishida, S.; Todo, H.; Iida, K.; Danjo, K. Stability of chitosan-pDNA complex powder prepared by supercritical carbon dioxide process. *Int. J. Pharm*. **2005**, *290*, 73−81.

(15) Kazarian, S. G.; Martirosyan, G. G. Spectroscopy of polymer/drug formulations processed with supercritical fluids: in situ ATR−IR and Raman study of impregnation of Ibuprofen into PVP. *Int. J. Pharm.* **2002**, *232*, 81−90.

(16) Wang, S.; Klenzle, F. The synthesis of pharmaceutical intermediates in supercritical fluids. *Ind. Eng. Chem. Res.* **2000**, *39*, 4487−4490.

(17) Russell, A. J.; Beckman, E. J.; Chaudhary, A. K. Studying enzyme activity in supercritical fluids. *CHEMTECH* **1994**, *24*, 33−38.

(18) Aaltonen, O. Rantakylä, M. Biocatalysis in supercritical CO_2. *CHEMTECH* **1991**, *21*, 240−248.

(19) Dhingra, V.; Vishweshwar Rao, K.; Lakshmi Narasu, M. Artemisinin: present status and perspectives. *Biochem. Educ.* **1999**, *27*, 105−109.

(20) Dhingra, V.; Vishweshwar Rao, K.; Lakshmi Narasu, M. Current status of artemisinin and its derivatives as antimalarial drugs. *Life Sci.* **2000**, *66(4)*, 279−300.

(21) Balint, G. A. Artemisinin and its derivatives: an important new class of antimalarial agents. *Pharmacol. Ther.* **2001**, *90*, 261−265.

(22) Meshnick, S. R. Artemisinin: mechanisms of action, resistance and toxicity. *Int. J. Parasitol.* **2002**, *32*, 1655−1660.

(23) Newton, P.; White, N. Malaria: new developments in treatment and prevention. *Annu. Rev. Med.* **1999**, *50*, 179−192.

(24) Galal, A. M.; Ross, S. A.; Jacob, M.; ElSohly M. A. Antifungal activity of artemisinin derivatives. *J. Nat. Prod.* **2005**, *68*, 1274−1276.

(25) Schmid, G.; Hofheinz, W. Total synthesis of Quinghaosu. *J. Am. Chem. Soc.* **1983**, *105*, 624−625.

(26) Avery, M. A.; Chong, W. K. M.; Jennings-White, C. Stereoselective total synthesis of (+)-artemisinin, the antimalarial constituent of *Artemisia annua* L. *J. Am. Chem. Soc.* **1992**, *114*, 974−979.

(27) Tang, Y.; Dong, Y.; Vennerstrom, J. L. Synthetic peroxides as antimalarials. *Med. Res. Rev.* **2004**, *24(4)*, 425−448.

(28) Ensenrik, M. Malaria researchers wait for industry to join fight. *Science* **2000**, *287*, 1956−1958.

(29) ElSohly, H. N.; Croom, E. M., Jr.; El-Feraly, F. S.; El-Sherei, M. M. A large scale extraction technique of artemisinin from *Artemisia annua*. *J. Nat. Prod.* **1990**, *53* (6), 1560−1564.

(30) Van Geldre, E.; Vergauwe, A.; Van den Eeckhout, E. State of the art of the production of the antimalarial compound artemisinin in plants. *Plant Mol. Biol.* **1997**, *33*, 199−209.

(31) Christen, P.; Veuthey, J.-L. New trends in extraction, identification and quantification of artemisinin and its derivatives. *Curr. Med. Chem.* **2001**, *8*, 1827−1839.

(32) Hao, J.; Han, W.; Huang, S.; Xue, B.; Deng, X. Microwave-assisted extraction of artemisinin from *Artemisia annua* L. *Sep. Purif. Technol.* **2002**, *28*, 191−196.
(33) Kohler, M.; Haerdi, W.; Christen, P.; Veuthey, J.-L. Supercritical fluid extraction and chromatography of artemisinin and artemisinic acid. An improved method for the analysis of *Artemisia annua* samples. *Phytochem. Anal.* **1997**, *8*, 223−227.
(34) Kohler, M.; Haerdi, W.; Christen, P.; Veuthey, J.-L. Extraction of artemisinin and artemisinic acid from *Artemisia annua* L. using supercritical carbon dioxide. *J. Chromatogr. A* **1997**, *785*, 353−360.
(35) Matias, A.; Nunes, A.; Casimiro, T.; Duarte, C. Solubility of coenzyme Q10 in supercritical carbon dioxide. *J. Supercrit. Fluids* **2004**, *28*(2−3), 201−206.
(36) Duarte, A. R.; Coimbra, P.; de Sousa, H. C.; Duarte, C. M. Solubility of flurbiprofen in supercritical carbon dioxide. *J. Chem. Eng. Data* **2004**, *49*, 449−452.
(37) Alessi, P.; Cortesi, A.; Kikic, I.; Foster, N. R.; Macnaughton, S. J.; Colombo, I. Solubility of anti-inflammatory drugs in supercritical carbon dioxide. *Ind. Eng. Chem. Res.* **2000**, *39*, 4794−4802.
(38) Bristow, S.; Shekunov, Y.; York, P. Solubility analysis of drug compounds in supercritical carbon dioxide using static and dynamic extraction systems. *Ind. Eng. Chem. Res.* **2001**, *40*, 1732−1739.
(39) Asghari-Khiavi, M.; Yamani, Y. Solubility of the drugs bisacodyl, methimazole, methylparaben, and iodoquinol in supercritical carbon dioxide. *J. Chem. Eng. Data* **2003**, *48*, 61−65.
(40) Knez, Ž.; Šerget, M.; Senčar-Božič, P.; Rižner, A. Solubility of nifedipine and nitrendipine in supercritical CO_2. *J. Chem. Eng. Data* **1995**, *40*, 216−220.
(41) Suleiman, D.; Estévez, L. A.; Pulido, J. C.; Garcia, J. E.; Mojica, C. Solubility of anti-inflammatory, anti-cancer, and anti-HIV drugs in supercritical carbon dioxide. *J. Chem. Eng. Data* **2005**, *50*, 1234−1241.
(42) Burgos-Solórzano, G. I.; Brennecke, J. F. Solubility measurements and modeling of molecules of biological and pharmaceutical interest with supercritical CO_2. *Fluid Phase Equilib.* **2004**, *220*, 57−69.
(43) Chrastil, J. Solubility of solids and liquids in supercritical gases. *J. Phys. Chem.* **1982**, *86*, 3016−3021.
(44) Bartle, K. D.; Clifford, A. A.; Jafar, S. A.; Shilstone, G. F. Solubilities of solids and liquids of low volatility in supercritical carbon dioxide. *J. Phys. Chem. Ref. Data* **1991**, *20* (4), 713−756.
(45) Méndez-Santiago, J.; Teja, A. S. Solubility of solids in supercritical fluids: consistency of data and a new model for cosolvent systems. *Ind. Eng. Chem. Res.* **2000**, *39*, 4767−4771.
(46) Jouyban, A.; Chan, H.-K.; Foster, N. R. Mathematical representation of solute solubility in supercritical carbon dioxide using empirical expressions. *J. Supercrit. Fluids* **2002**, *24*, 19−35.
(47) Hartono, R.; Mansoori, G. A.; Suwomo, A. Prediction of solubility of biomolecules in supercritical solvents. *Chem. Eng. Sci.* **2001**, *56*, 6949−6958.
(48) Ashour, I.; Almehaideb, R.; Fateen, S. E.; Aly, G. Representation of solid-supercritical fluid phase equilibrium using cubic equations of state. *Fluid Phase Equilib.* **2000**, *167*, 41−61.
(49) Garnier, S.; Neau, E.; Alessi, P.; Cortesi, A.; Kikic, I. Modeling solubility of solids in supercritical fluids using fusion properties. *Fluid Phase Equilib.* **1999**, *158*−*160*, 491−500.
(50) Ziger, D. H.; Eckert, C. Correlation and prediction of solid-supercritical phase equilibria. *Ind. Eng. Chem. Proc. Des. Dev.* **1983**, *22*, 582−588.
(51) Coimbra, P.; Duarte, C. M. M.; de Sousa, H. C. Cubic equation-of-state correlation of the solubility of some anti-inflammatory drugs in supercritical carbon dioxide. *Fluid Phase Equilib.* **2006**, *229*, 188−199.
(52) Coimbra, P.; Gil, M. H.; Duarte, C. M. M.; Heron, B. M.; de Sousa, H. C. Solubility of a spiroindolinonaphthoxazine photochromic dye in supercritical carbon dioxide: experimental determination and correlation. *Fluid Phase Equilib.* **2005**, *238*, 120−128.
(53) Robinson, D. B.; Peng, D.-Y. A new two-constant equation of state. *Ind. Eng. Chem. Fundam.* **1976**, *15(1)*, 59−64.
(54) Soave, G. Equilibrium constants from a modified Redlich−Kwong equation of state. *Chem. Eng. Sci.* **1972**, *27*, 1197−1203.
(55) Xing, H.; Yang, Y.; Su, B.; Huang, M.; Ren, Q. Solubility of artemisinin in supercritical carbon dioxide. *J. Chem. Eng. Data* **2003**, *48* (2), 330−332.
(56) Fujiwara, S.-i.; Yamashita, F.; Hashida, M. Prediction of Caco-2 cell permeability using a combination of MO-calculation and neural network. *Int. J. Pharm.* **2002**, *237*, 95−105.
(57) Kazarian, S. G.; Vincent, M. F.; Bright, F. V.; Liotta, C. L.; Eckert, C. A. Specific intermolecular interaction of carbon dioxide with polymers. *J. Am. Chem. Soc.* **1996**, *118*, 1729−1736.
(58) Kazarian, S. G.; Brantley, N. H.; West, B. L.; Vincent, M. F.; Eckert, C. A. In situ spectroscopy of polymers subjected to supercritical CO_2: plasticization and dye impregnation. *Appl. Spectrosc.* **1997**, *51*, 491−494.
(59) Kazarian, S. G. Polymer processing with supercritical fluids. *Polym. Sci., Ser. C* **2000**, *42* (1), 78−101.
(60) Buckingham, A. D.; Disch, R. L. Quadropole moments of some simple molecules. *J. Am. Chem. Soc.* **1968**, *90*, 3104−3107.
(61) Poling, B. E.; Prausnitz, J. M.; O'Connell, J. P. *The Properties of Gases and Liquids*, 5th ed.; McGraw-Hill: New York, 2001.
(62) Fedors, R. A. Method for estimating both the solubility parameters and molar volume of liquids. *Polym. Eng. Sci.* **1974**, *14(2)*, 147−154.

Received for review January 11, 2006. Accepted March 30, 2006. This work was financially supported by FCT-MCES and FEDER, Portugal, under Contract POCTI/FCB/38213/2001.

JE060015Y